ARMY RESEARCH LABORATORY

Ultrasound-assisted Micro-emulsion Synthesis of a Highly Active Nano-particle Catalyst

by Rongzhong Jiang and Charles Rong

ARL-TR-5114 **March 2010**

NOTICES

Disclaimers

The findings in this report are not to be construed as an official Department of the Army position unless so designated by other authorized documents.

Citation of manufacturer's or trade names does not constitute an official endorsement or approval of the use thereof.

Destroy this report when it is no longer needed. Do not return it to the originator.

Army Research Laboratory
Adelphi, MD 20783-1197

ARL-TR-5114 **March 2010**

Ultrasound-assisted Micro-emulsion Synthesis of a Highly Active Nano-particle Catalyst

Rongzhong Jiang and Charles Rong
Sensors and Electron Devices Directorate, ARL

REPORT DOCUMENTATION PAGE

Form Approved
OMB No. 0704-0188

1. REPORT DATE *(DD-MM-YYYY)*	2. REPORT TYPE	3. DATES COVERED (From - To)
March 2010	DRI	2009 to 2010

4. TITLE AND SUBTITLE
Ultrasound-assisted Micro-emulsion Synthesis of a Highly Active Nano-particle Catalyst

5a. CONTRACT NUMBER

5b. GRANT NUMBER

5c. PROGRAM ELEMENT NUMBER

6. AUTHOR(S)
Rongzhong Jiang and Charles Rong

5d. PROJECT NUMBER

5e. TASK NUMBER

5f. WORK UNIT NUMBER

7. PERFORMING ORGANIZATION NAME(S) AND ADDRESS(ES)
U.S. Army Research Laboratory
ATTN: RDRL-SED-C
2800 Powder Mill Road
Adelphi, MD 20783-1197

8. PERFORMING ORGANIZATION REPORT NUMBER
ARL-TR-5114

9. SPONSORING/MONITORING AGENCY NAME(S) AND ADDRESS(ES)

10. SPONSOR/MONITOR'S ACRONYM(S)

11. SPONSOR/MONITOR'S REPORT NUMBER(S)

12. DISTRIBUTION/AVAILABILITY STATEMENT
Approved for public release; distribution unlimited.

13. SUPPLEMENTARY NOTES

14. ABSTRACT
Several wet chemical methods were examined for synthesis of platinum (Pt) and Pt-cobalt (Co) nano-particles, including normal chemical synthesis, micro-emulsion synthesis, and ultrasound-assisted micro-emulsion synthesis. High resolution transmission electron microscopy (TEM), x-ray diffraction analysis (XRD), and electrochemical methods were used for characterization of the synthesized catalysts. The Pt-Co synthesized with ultrasound-assisted micro-emulsion showed uniform particle size distribution. The particle size was well controlled from 17 to 3 nm by varying the water/oil ratio, the water/surfactant ratio, the reactant concentration, and the pH value in the water phase. Several electrochemical methods were used to characterize the catalytic activity for oxygen reduction. The Pt-Co nano-particles synthesized with ultrasound-assisted micro-emulsion showed significantly higher catalytic activity for oxygen reduction than those synthesized with other wet chemical methods. It was able to catalyze oxygen 4-electron reduction to water at an onset potential about 0.65 V (vs. saturated calomel electrode [SCE]).

15. SUBJECT TERMS
Microemulsion synthesis, Nano particles, Catalysts, Ultrasound, Oxygen reduction, Rotating disk electrode

16. SECURITY CLASSIFICATION OF:			17. LIMITATION OF ABSTRACT	18. NUMBER OF PAGES	19a. NAME OF RESPONSIBLE PERSON
a. REPORT	b. ABSTRACT	c. THIS PAGE			Rongzhong Jiang
Unclassified	Unclassified	Unclassified	UU	40	19b. TELEPHONE NUMBER (*Include area code*) (301) 394-0295

Standard Form 298 (Rev. 8/98)
Prescribed by ANSI Std. Z39.18

Contents

List of Figures

List of Tables

Acknowledgments

We wish to thank Dr. Wendy Sarney at the U.S. Army Research Laboratory (ARL) and Professor Chunsheng Wang at the University of Maryland for providing transmission electron micrograph (TEM) analysis.

INTENTIONALLY LEFT BLANK.

1. Objective

The objective of this Director's Research Initiative (DRI) is to develop innovative synthetic methods for realizing uniformly distributed nano-sized metal alloy particles using an interdisciplinary approach that employs physics, chemistry, and material science techniques. The proposed method will enable us to produce a new metal-based catalyst that exhibits high reactivity for fuel oxidation and oxygen reduction in both alkaline and acid electrolytes for high energy and high power fuel cells.

2. Approach

2.1 Background

Energy consumption plays an important role in our modern civilization and daily life, which is heavily dependent on burning fossil fuels. The increasing threat of the fast depletion of resources such as petroleum, coal, and natural gas, and, in turn, the green house effect caused by burning fossil fuels, forces people to seek regenerative energy sources, such as solar, wind, geothermal, and hydroelectric energies. An alternative way to save valuable natural resources and solve the environmental problem is to develop cleaner and more efficient energy conversion devices. In recent years, fuel cell research and development have received much attention (*1–8*) for creating higher energy conversion efficiency and lower or no greenhouse gas emissions in their processes for converting fuel into usable energies. The power and energy efficiency of a fuel cell is highly dependent on the fuel cell's thermodynamics, electrode kinetics, and reactant mass transfer, as well as the materials and components used to assemble the fuel cell. One of the most important materials for making a fuel cell is electrode catalysts for oxygen reduction and fuel oxidation. Unfortunately, so far, practical fuel cells still rely on using expensive noble metals as catalysts. One way to efficiently use noble metals as catalysts is to reduce the metal particles to nano size and increase the surface area of the catalyst to allow more fuel or oxygen molecules to access the active sites on the surface of the catalyst. There are many technologies for synthesizing fuel cell catalysts (*9–22*), such as direct chemical reduction, impregnation, co-precipitation, colloidal, and micro-emulsion methods. The simplest method is direct chemical reduction, which often results in large or non-nano-sized metal particles. In the impregnation method, platinum (Pt) and transition metal precursors are first adsorbed on a carbon support and subsequently the mixture is dried and reduced with a hydrogen stream at 200 to 700 °C in a tubular furnace. The high temperature of the hydrogen stream drives the reduction to completion. The disadvantage is that the high temperature decreases the active surface area because of the aggregation of the nano-particles. In the co-precipitation method, the platinum halide and transition metal oxide are mixed with an excess of sodium nitride and heated to 500 °C for a few hours. Then the solidified

melt is washed with water to remove nitrate and chloride, and reduced by hydrogen gas between room temperature and 200 °C. In the colloidal method, surfactant or polymer is often used as stabilizers to protect the nano-sized particles from recombination and the reduction temperature is well below 200 °C. However, it has been discovered that the conditions of colloidal method also create a space for the nano-particle to grow, which is a main limiting factor to obtaining smaller nano-particle size in this method. Additionally, removing the stabilizer after reduction becomes a major concern.

2.2 Approach

Micro-emulsion (*21–25*) is a synthetic method developed in recent years for synthesizing nano-sized metal or non-metal particles, which also uses surfactant as a stabilizer, but does not leave space for nano-particles to grow. A micro-emulsion consists of nano-sized water droplets surrounded by an organic phase and stabilized by a surfactant. This method can be used to synthesize metal catalysts for fuel cell applications. In micro-emulsion synthesis, one or more metal salts can be dissolved in the nano-sized water domain and reduced to metals or alloys with a chemical reducing reagent. Because of the space limitation in the water droplet, the growth of crystalline particles is restricted. The particle size distribution of the catalyst through common micro-emulsion is distributed over a relative large area because the water droplets in the synthetic process are not well controlled. We found that by introducing ultrasound into the environment, the micro-emulsion was able to distribute the catalyst particle size more uniformly. The ultrasonic method is rarely used in synthesis of nano metal catalysts. In this one-year DRI research, we focused on synthesis of Pt-cobalt (Co) catalysts for oxygen reduction. It was reported (*22–27*) that alloyed Pt-Co demonstrated higher catalytic activity than Pt alone for oxygen reduction. The micro-emulsion assisted with ultrasound was also proposed to synthesize a variety of other catalysts, including those needed for catalytic fuel oxidation. Figure 1 shows the principle of micro-emulsion for synthesis of nano metal particles.

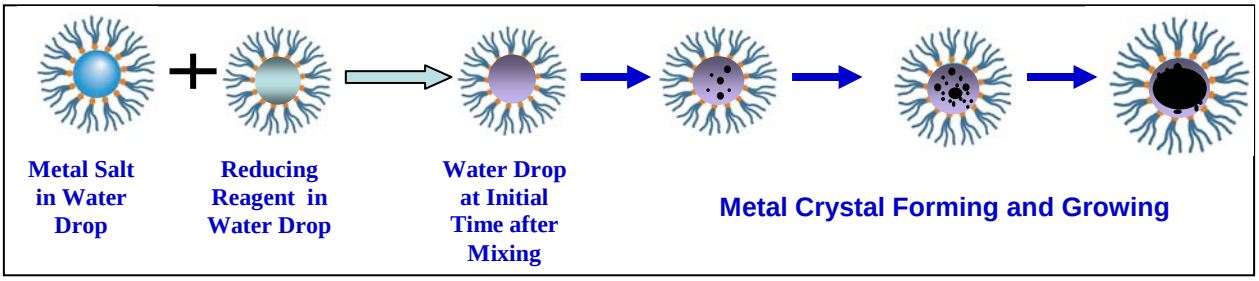

Figure 1. Schematic drawing of micro-emulsion for the synthesis of a metal alloy.

2.3 Experimental Methods and Procedures

In order to develop a highly active Pt-Co catalyst, we first needed to choose a synthetic method. Secondly, we needed to determine the catalytic activity of catalysts synthesized with different methods. Therefore, we needed to experimentally compare different synthetic methods to identify which one resulted in the best catalyst. The following is a summary of the synthetic methods and instrumental analyses used in our experiments.

2.3.1 Normal Chemical Synthesis (NCS)

First, 1.0 g of hydrogen hexachloro-platinum pentahydrate ($H_2PtCl_6 \cdot 5H_2O$) and an appropriate amount of cobalt (II) chloride hexahydrate ($CoCl_2 \cdot 6H_2O$) were dissolved in 100 mL of water in a 1000-mL flask. Then, 10 mL of ammonium hydroxide (NH_4OH) water was added into it to form ammonia metal complexes. The mixture was stirred, and then we added a 20 times excess of powdered sodium borohydride ($NaBH_4$) as a reducing reagent into it slowly. The reaction was completed in about 2 h under nitrogen (N_2) atmosphere, where the N_2 gas was introduced into the flask above the solution surface. Black precipitate was formed slowly in the solution. After reaction, the black precipitate was separated by filtration and washed with water for about 4 h. The black powder of Pt-Co alloy was collected and dried in a vacuum oven at 40 °C overnight.

2.3.2 Micro-emulsion in High pH Environment (ME-H)

The reaction was maintained in a weak base environment buffered with ammonia water. The following steps were used to synthesize nano Pt-Co catalyst using the ME-H method:

- *Solution A*: First, 1.0 g of H_2PtCl_6 $5H_2O$ and an appropriate amount of $CoCl_2$ $6H_2O$ were dissolved in a small amount of water in a 1000-mL flask. Then, 10 mL of NH_4OH water was added into it to form ammonia metal complexes. Next, 40 mL of Brij 30 (polyethylene glycol dodecyl ether, polyoxyethylene (4) layryl ether, or $[C_{20}H_{42}O_5]_n$) was added and stirred vigorously to form a uniform gel. Finally, 140 mL of heptane was added into the gel and stirred until it was fully dissolved.
- *Solution B*: First, 1.8 g of $NaBH_4$ and 2 mL of NH_4OH were dissolved into a small amount of water. Next, 10 mL of Brij was added to form a gel. Then, 90 mL of heptane was added into it. The mixture was stirred until the solution became clear.
- *Reaction and precipitate step*: Solution B was filled into a stopcock funnel and slowly dropped into the reaction flask containing solution A. The reaction was completed in about 2 to 3 h under N_2 atmosphere. The solution gradually turned black during reaction. Then, 300 mL of ethanol was added into the flask to destruct the micro-emulsion and precipitate the nano-sized Pt-Co from the liquid. Figure 2 shows images of the process in micro-emulsion synthesis of Pt-Co catalyst.

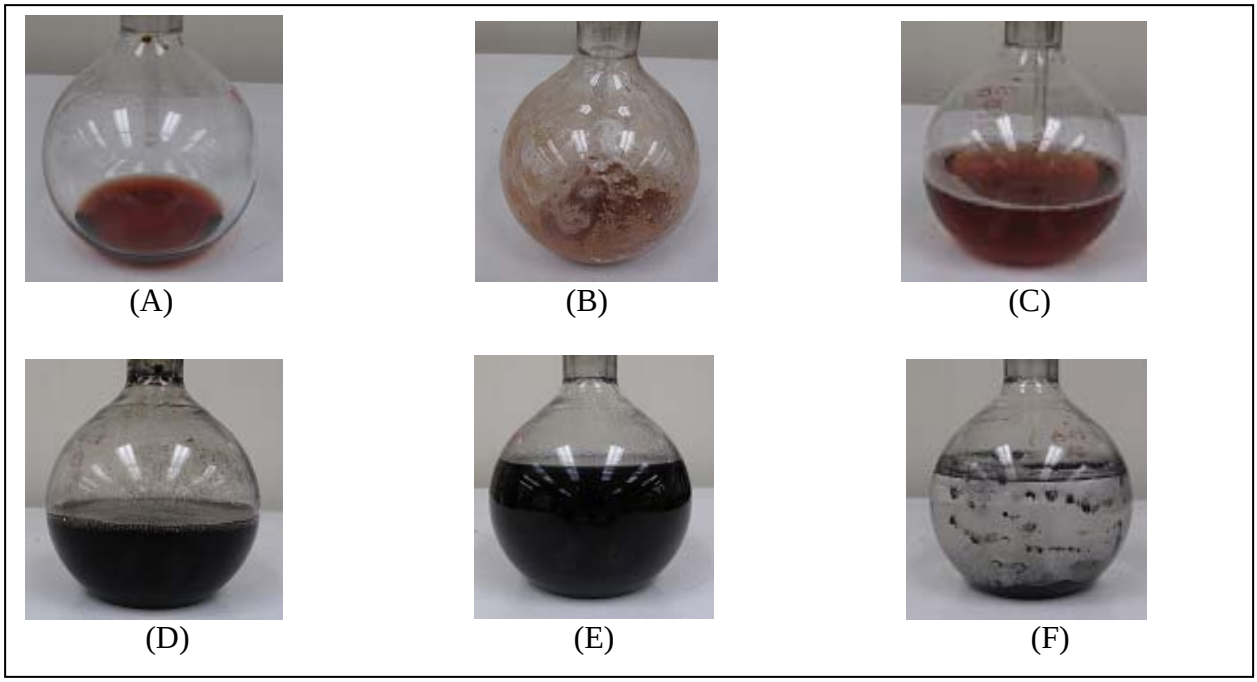

Figure 2. Images of the process in micro-emulsion synthesis of Pt-Co catalyst: (a) mixing the Pt and Co compounds; (b) after adding the chemical surfactant; (c) adding the oil to form the micro-emulsion; (d) adding a reducing reagent to form the Pt-Co alloy; (e) adding ethanol to precipitate the Pt-Co particles; and (f) after standing overnight.

- *Separation and wash step*: The black precipitate in the liquid was separated by filtration under vacuum condition. Then, it was washed with water and ethanol, alternatively, many times until no bubbles were seen in the filtrate. The black power of Pt-Co was collected and dried in a vacuum oven at 40 °C overnight.

2.3.3 Micro-emulsion in Low pH Environment (ME-L)

The same steps were followed as with ME-H, except no NH_4OH was added to the reaction solution and the reducing reagent, $NaBH_4$, was replaced by hydrazine (also at a 20 times excess).

2.3.4 Ultrasound-assisted Micro-emulsion in High pH Environment (U-ME-H)

The same steps were followed as with ME-H, except the reaction was carried out in an ultrasonic bath (Branson 3510).

2.3.5 Ultrasound-assisted Micro-emulsion in Low pH Environment (U-ME-L)

The same steps were followed as with ME-L, except the reaction was carried out in an ultrasonic bath (Branson 3510).

2.3.6 Sub-synthetic Methods

In addition to the five basic synthetic methods described previously, there were several sub-methods used to optimize particle size and the catalytic performance of Pt-Co, such as (1) adjusting the ratio of Pt and Co in the alloy for better catalytic activity, (2) lowering the metal salt (H_2PtCl_6) concentration for a smaller Pt-Co particle size, (3) lowering the ratio of water to oil for smaller water droplets in the micro-emulsion, (4) adding carbon (XC72R) for better distribution of the nano metal particles, and (5) using a heat treatment to remove the residue surfactant in the catalyst after synthesis. These synthetic methods are summarized in table 1.

Table 1. Summary of synthetic methods used for the preparation of nano Pt-Co catalysts.

Synthetic Method	Water/Oil Ratio (v/v)	Water/Brij Ratio (v/v)	H_2PtCl_6 in Water Phase (mM)	Reducing Reagent	Ultrasonic Bath	NH_4OH Buffered
NCS	N/A	N/A	1.8	$NaBH_4$	No	Yes
ME-H	1:5	3:4	6.7	$NaBH_4$	No	Yes
U-ME-H1	1:5	3:4	6.7	$NaBH_4$	Yes	Yes
U-ME-H2	1:50	1:10	4.0	$NaBH_4$	Yes	Yes
30%C U-ME-H1	1:5	3:4	6.7	$NaBH_4$	Yes	Yes
30% C U-ME-H2	1:50	1:10	4.0	$NaBH_4$	Yes	Yes
30%C U-ME-L1	1:5	3:4	6.7	Hydrazine	Yes	No
30% C U-ME-L2	1:50	1:10	4.0	Hydrazine	Yes	No

2.3.7 Electrochemical Analysis

Pine Bipotentiostat RDE4 was used for the electrochemical analysis of the synthesized nano Pt-Co catalysts. Firstly, 20 mg of catalyst sample was processed to an ink by adding 2 mL of water, 2 mL of ethanol, and 0.2 g of 5% Nafion, and using an ultrasonic treatment with a Branson 450 Sonifier. Then, 5 µl of catalyst ink was coated on a glassy carbon (GC) rotating disk electrode (Pine E7R9 GC [0.247 cm^2], Pt ring electrode, Collection Efficiency 0.37), and dried at 30 °C under vacuum for 3 h or more. The catalyst loading was about 0.1 mg/cm^2. The catalyst-coated electrode was mounted onto Pine Adjustable Speed Rotator (ASR) and measured in 0.5 M of sulfuric acid (H_2SO_4) at room (20 ± 1 °C) under an oxygen (O_2) or N_2 saturated condition, respectively. The Pt-Co coated GC was the working electrode, the platinum wire was the counter electrode, and the saturated calomel was the reference electrode. The catalytic activity of the catalyst was obtained by cyclic voltammetry (CV), rotating disk electrode (RDE), and rotating ring disk electrode (RRDE) measurements.

2.3.8 Transmission Electron Microscope (TEM) Image

CF400-Cu Carbon film (Electron Microscopy Science) was used to load the TEM sample. First, we dispersed 10 mg of nano-catalyst powder Pt-Co into a solution containing 1 mL of water and 1 mL of ethanol. The mixture was placed in a small glass vial and treated in an ultrasonic bath (Branson 3510) for a few minutes until a satisfactory ink was obtained. About 1 µL of ink was loaded onto the CF400-Cu with a micro pipette. After this, the sample was dried overnight at

room temperature. A TEM image was obtained using a high resolution JEOL 2100 FEG TEM instrument. In addition, energy dispersive x-ray spectroscopy (EDS) analysis was obtained using the same instrument.

2.3.9 X-Ray Diffraction Analysis (XRD)

XRD results were obtained using a Rigaku Ultima III instrument with Cu Kα radiation ($\lambda = 1.5418$ Å) using a Bragg-Brentano configuration. The measurements were conducted with scan rate of 0.1 degree (2θ) per min and each diffraction data point was collected at the interval of 0.03 degree (2θ). The total spectrum range was from 30 to 100 degree (2θ).

3. Results

3.1 TEM Images

The particle size of Pt-Co catalyst synthesized by the ultrasound-assisted micro-emulsion was examined using high resolution TEM. Figure 3 shows the TEM images of Pt-Co catalysts synthesized by ultrasound-assisted micro-emulsion with a Pt/Co ratio of 7:3, a water/oil ratio of 1:5, and an H_2PtCl_6 concentration in water phase of 6.7 mM. The particle size was distributed uniformly at 17 nm. There was no apparent difference of particle size between the unsupported Pt-Co and the 30% carbon supported Pt-Co. It was unexpected that addition of carbon powder in the process for synthesizing Pt-Co did not reduce the metal particle size. EDS analysis was also carried out. Tables 2 and 3 show the EDS analysis of TEM samples of the unsupported and carbon supported Pt-Co that were synthesized by ultrasound-assisted micro-emulsion with a Pt/Co ratio of 7:3, a water/oil ratio of 1:5, and an H_2PtCl_6 concentration in water phase of 6.7 mM. The atomic ratio of Pt to Co matches closely with the expected 7:3 ratio (or Pt/(Pt+Co) = 0.70).

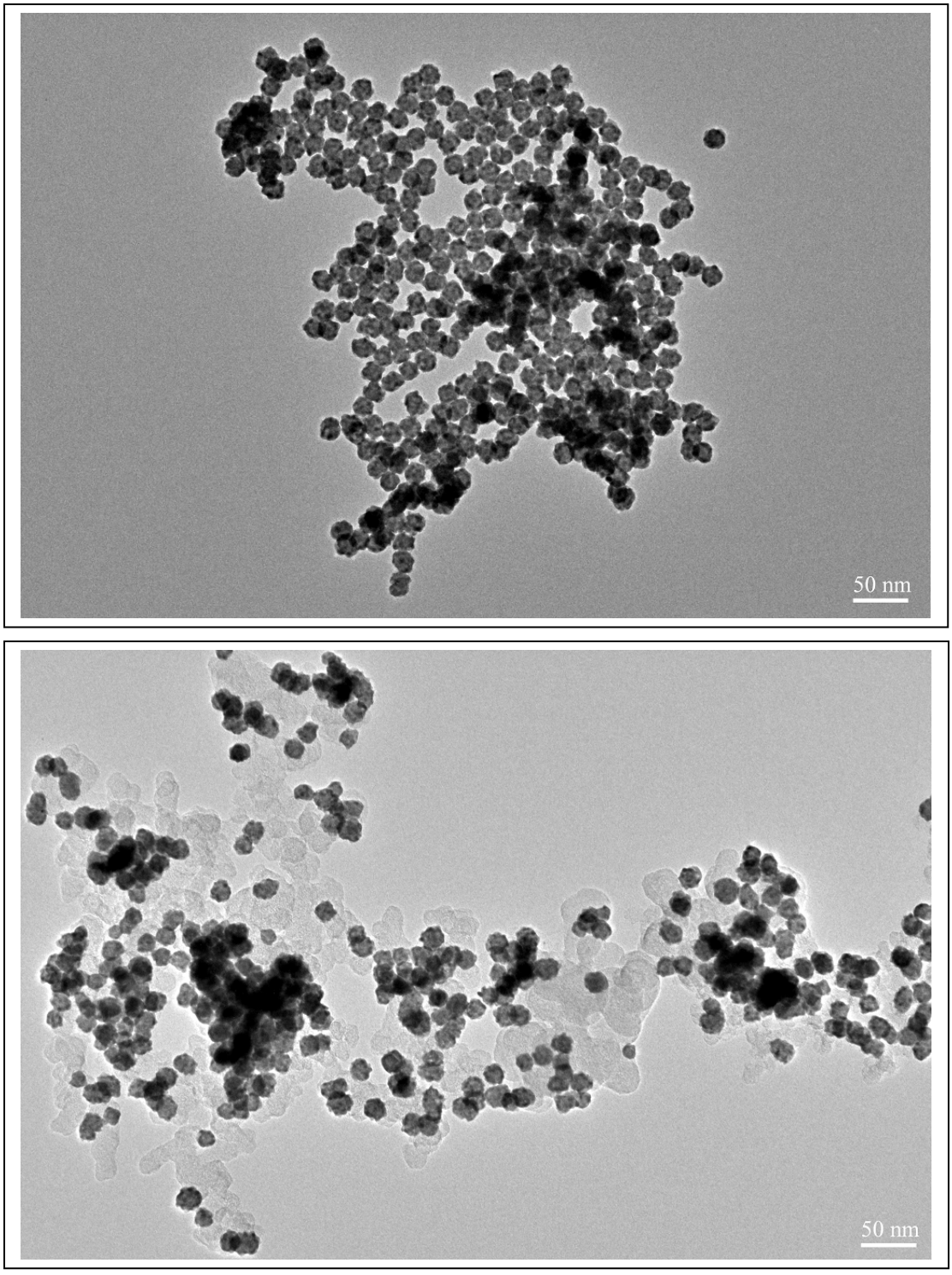

Figure 3. TEM images of Pt-Co catalysts synthesized by ultrasound-assisted micro-emulsion with a Pt/Co ratio of 7:3, a water/oil ratio of 1:5, and an H_2PtCl_6 concentration in water phase of 6.7 mM: (top) unsupported Pt-Co and (bottom) 30% carbon supported Pt-Co. The particle size was 17 nm.

Table 2. EDS analysis of the TEM sample of unsupported Pt-Co that was synthesized by ultrasound-assisted micro-emulsion with a Pt/Co ratio of 7:3, a water/oil ratio of 1:5, and an H_2PtCl_6 concentration in water phase of 6.7 mM.

Element	Weight%	Atomic%	Atomic Ratio
C	16.82	61.36	–
Co	3.92	2.91	–
Cu	38.56	26.58	–
Pt	40.70	9.14	–
Pt/(Co+Pt)	–	–	0.76
Totals	100	100	–

Table 3. EDS analysis of the TEM sample of the 30% XC72R carbon supported Pt-Co that was synthesized by ultrasound-assisted micro-emulsion with a Pt/Co ratio of 7:3, a water/oil ratio of 1:5, and an H_2PtCl_6 concentration in water phase of 6.7 mM.

Element	Weight%	Atomic%	Atomic Ratio
C	37.14	84.89	–
O	2.74	4.71	–
Co	5.98	2.78	–
Pt	54.15	7.62	–
Pt/(Co+Pt)	–	–	0.73
Totals	100	100	–

To attempt to reduce the Pt-Co particle size, we tried to decrease the metal salt concentrations of the H_2PtCl_6 from 6.7 to 4.0 mM in the water droplet and to decrease the water/oil ratio from 1:5 to 1:50. The particle size of Pt-Co was significantly decreased from 17 to 10 nm. The upper figure in figure 4 shows the TEM image of the Pt-Co catalysts synthesized by ultrasound-assisted micro-emulsion with a Pt/Co ratio of 7:3, a water/oil ratio of 1:50, and an H_2PtCl_6 concentration in water phase of 4.0 mM. The EDS analysis does not show appreciable change in the Pt-to-Co ratio after changing the water/oil ratio and the H_2PtCl_6 concentration in the synthetic process, as shown in table 4. Further reducing the particle size to 3 nm was achieved by replacing the reducing reagent from $NaBH_4$ to hydrazine, and avoiding using ammonia buffer in the water droplet. The lower figure in figure 3 shows the TEM image of the PtCo catalyst synthesized by ultrasound assisted micro-emulsion with a Pt/Co ratio of 7:3, a water/oil ratio of 1:50, and an H_2PtCl_6 concentration in water phase of 4.0 mM, using hydrazine as reducing reagent and without using ammonia buffer.

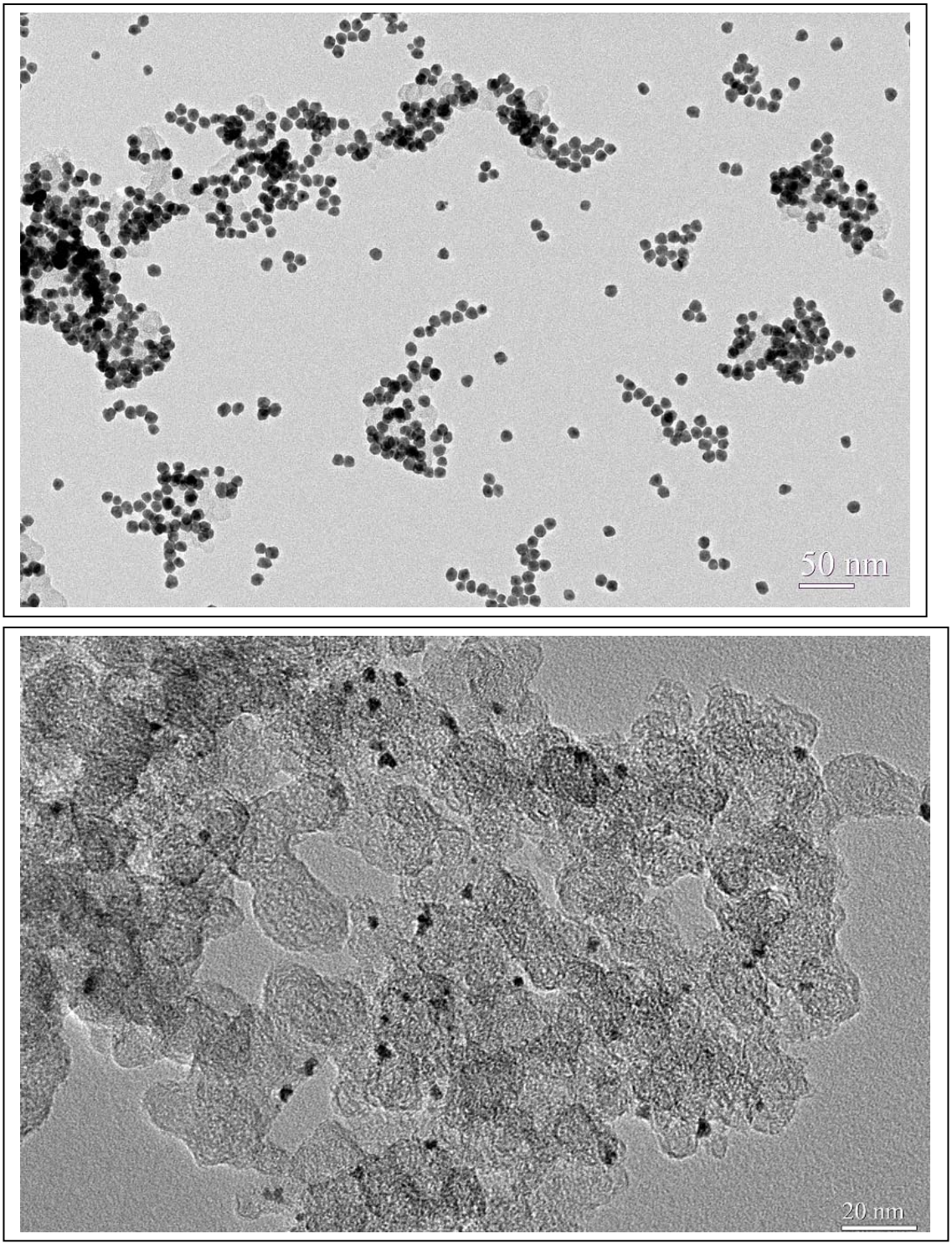

Figure 4. TEM images of the 30% carbon Pt-Co catalyst synthesized by ultrasound-assisted micro-emulsion with Pt/Co ratio of 7:3. (Top) Synthesized with the method of U-ME-H2 particle size: 10 nm and (bottom) synthesized with the method of U-ME-L2. The particle size is 3 nm.

Table 4. EDS analysis of the TEM sample of the 30% XC72R carbon supported Pt-Co that was synthesized by ultrasound-assisted micro-emulsion with a Pt/Co ratio of 7:3, a water/oil ratio of 1:50, and an H_2PtCl_6 concentration in water phase of 4.0 mM.

Element	Weight%	Atomic%	Atomic Ratio
C	71.04	95.02	–
O	2.28	2.29	–
Co	2.59	0.71	–
Pt	24.08	1.98	–
Pt/(Co+Pt)	–	–	0.74
Totals	100	100	–

3.2 XRD Analysis

Nano-sized samples of pure Pt and 7/3 Pt-Co alloy that were synthesized by the ultrasound-assisted micro-emulsion approach are shown in figure 5 compared to commercial Pt catalyst. The results of the synthesized and the commercial pure Pt are very similar, while the 7/3 Pt-Co alloy appears broadened in its diffraction patterns, which suggested a smaller crystalline size. This is in agreement with the TEM observation that the synthesized Pt-Co alloy has a polycrystalline phase within the particle size domain of about 17 nm.

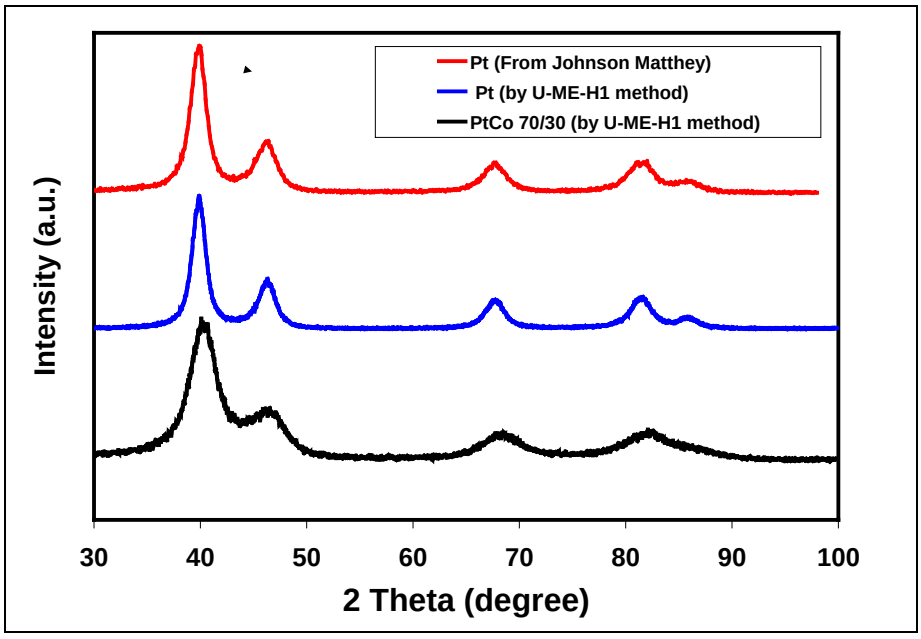

Figure 5. XRD results of pure Pt and Pt-Co alloy.

Further examination of the position of the diffraction patterns of the ultrasound-assisted micro-emulsion synthesized sample with the standard diffraction data of pure Pt and the known Pt-Co alloy $CoPt_3$ are listed in table 5. The sample of Pt-Co 7/3 falls in between the two standard, confirming that a Pt-Co alloy is, indeed, formed. Based on the XRD results, we anticipate that the samples may not be the single phase of $CoPt_3$ that needs further heat treatment for its complete formation.

Table 5. XRD peak positions of pure Pt and Pt-Co alloy.

Sample	Peak Position				
	Peak-1	**Peak-2**	**Peak-3**	**Peak-4**	**Peak-5**
Pt (087-0636)[a]	39.036	45.876	66.905	80.624	
PtCo 7/3	40.252	46.425	68.117	81.667	
$CoPt_3$ (029-0499) [a]	40.536	47.272	68.795	83.088	87.770

[a] Powder Diffraction File number from International Center for Diffraction Data.

Figure 6 summarized the XRD results of samples from three synthetic methods. Although they seemed to have virtually the same pattern, the electrochemical investigation demonstrated an improved reactivity toward oxygen reduction with the ultrasound-assisted micro-emulsion synthesized sample.

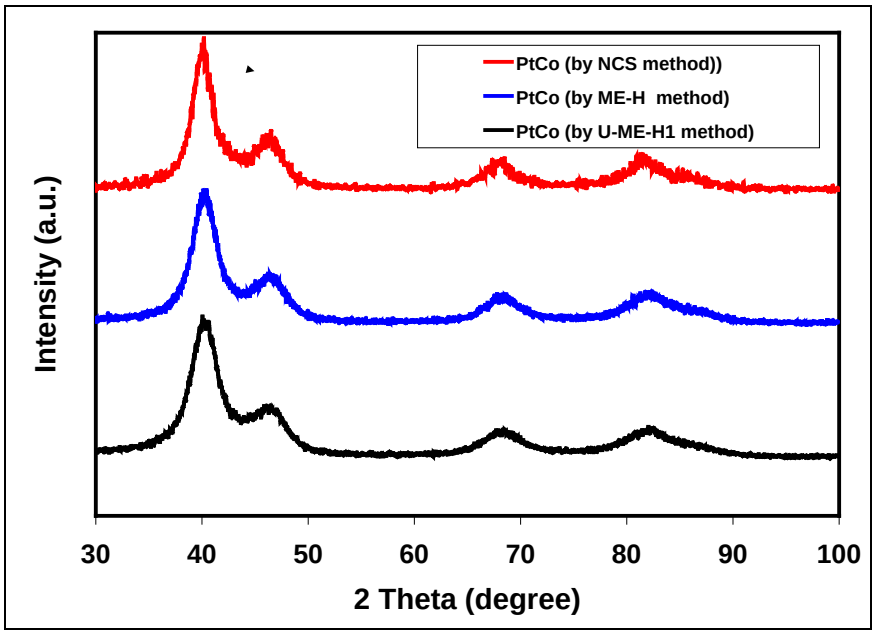

Figure 6. XRD results of Pt-Co alloy catalyst obtained with different synthetic methods. The PtCo ratio is 7:3.

3.3 Cyclic Voltammetry (CV)

The common widely used electrochemical method for characterization of electrode catalysts is CV. When a triangular potential-time wave is applied to the working electrode, a typical current response can be expressed with equation 1 for a reversible electrochemical reaction and with equation 2 for an irreversible electrochemical reaction (*28*), respectively.

$$i_p = (2.69\times10^5)n^{3/2}AD_o^{1/2}\upsilon^{1/2}C_o^* \quad (1)$$

$$i_p = (2.99\times10^5)n(\alpha n_\alpha)^{1/2}AC_o^*D_o^{1/2}\upsilon^{1/2} \quad (2)$$

Here, i_p is peak current (A), n is the electron number per molecule oxidized or reduced, and υ (V/s) is the linear potential scan rate. A is the electrode area (cm^2), D_o is the diffusion coefficient (cm^2/s) of species O, C_o^* (mol/cm^3) is the concentration of species O in the bulk solution, α is electron transfer coefficient, and n_α is the number of electrons involved in the rate determining step. As oxygen reduction belongs to an irreversible reaction, equation 2 is used to analyze the CV results. Oxygen reduction may follow different schemes to produce water or hydrogen peroxide, depending on different kinds of catalysts, as shown in equations 3 and 4.

$$O_2 + 4H^+ + 4e^- = 2H_2O \qquad E^o=1.23V \qquad (3)$$

$$O_2 + 2H^+ + 2e^- = H_2O_2 \qquad E^o= 0.69V \qquad (4)$$

We preferred that the catalytic reduction of oxygen followed scheme in equation 3 to obtain a higher fuel cell voltage and to avoid producing the harmful byproduct hydrogen peroxide, which is corrosive to electrodes and components.

3.3.1 Catalyst Synthesized with Ultrasound-assisted Micro-Emulsion

Figure 7 shows CVs of Pt-Co coated GC electrode (expressed as PtCo/GC) in N_2 and O_2 saturated 0.5 M H_2SO_4 solutions, respectively. In the absence of O_2, a typical cyclic voltammogram of a Pt electrode is shown. There are two reductive waves at +0.6 and –0.1 V, which belong to a platinum oxide reduction at the electrode surface and a catalytic proton reduction, respectively. In the presence of O_2, the first wave at +0.6 V grows significantly. The peak current in the presence of O_2 is about six times of that in the absence of O_2, and the peak potential is at about 0.6 V. This is a typical catalytic wave for oxygen reduction.

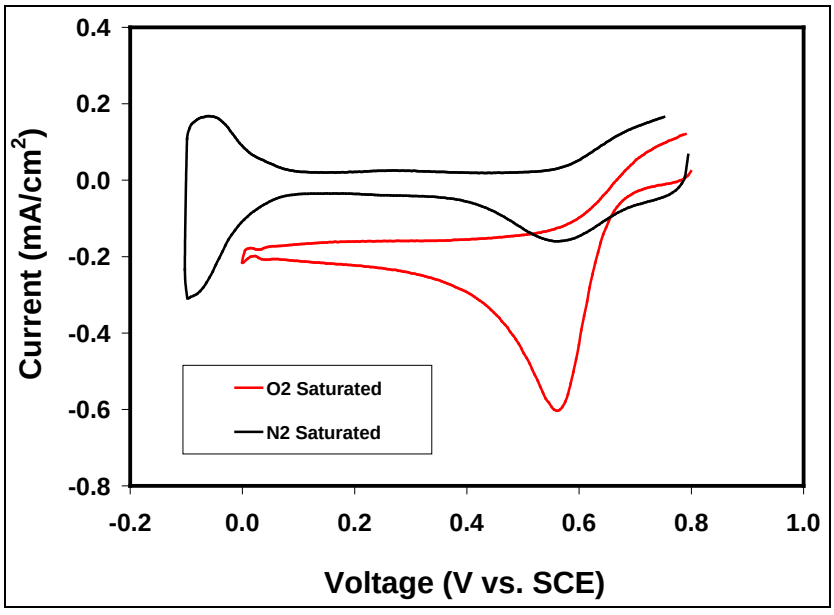

Figure 7. Cyclic voltammograms of PtCo/GC electrodes (Pt:Co = 7:3) in N_2 and O_2 saturated 0.5 M H_2SO_4 solutions, respectively. The scan rate is 10 mV/s. The PtCo was synthesized with ultrasound-assisted micro-emulsion.

The catalytic activity of the catalysts synthesized with and without ultrasound is compared. Figure 8 shows CVs of PtCo/GC electrodes, for which the catalysts were synthesized using the U-ME-H1 and ME-H methods, respectively. In a N_2 saturated solution, the wave at +0.6 V was not appreciable for the catalyst synthesized using ME-H, and the proton reduction/hydrogen oxidation wave at –0.1 V becomes smaller in comparison with the catalyst synthesized with the U-ME-H1 method. This phenomenon is due to some of the catalytic sites being inactive for the catalysts synthesized with the ME-H method. Applying ultrasound in the micro-emulsion synthesis environment may increase the kinetic reaction between reactants and reducing reagent to improve alloy formation, as well as distribute the particles more uniformly. In an O_2 saturated solution, the peak potential for the catalyst synthesized with ultrasound had 30-mV shift to positive, and the peak current showed an 80-$\mu A/cm^2$ increase in comparison with the catalyst synthesized without using ultrasound.

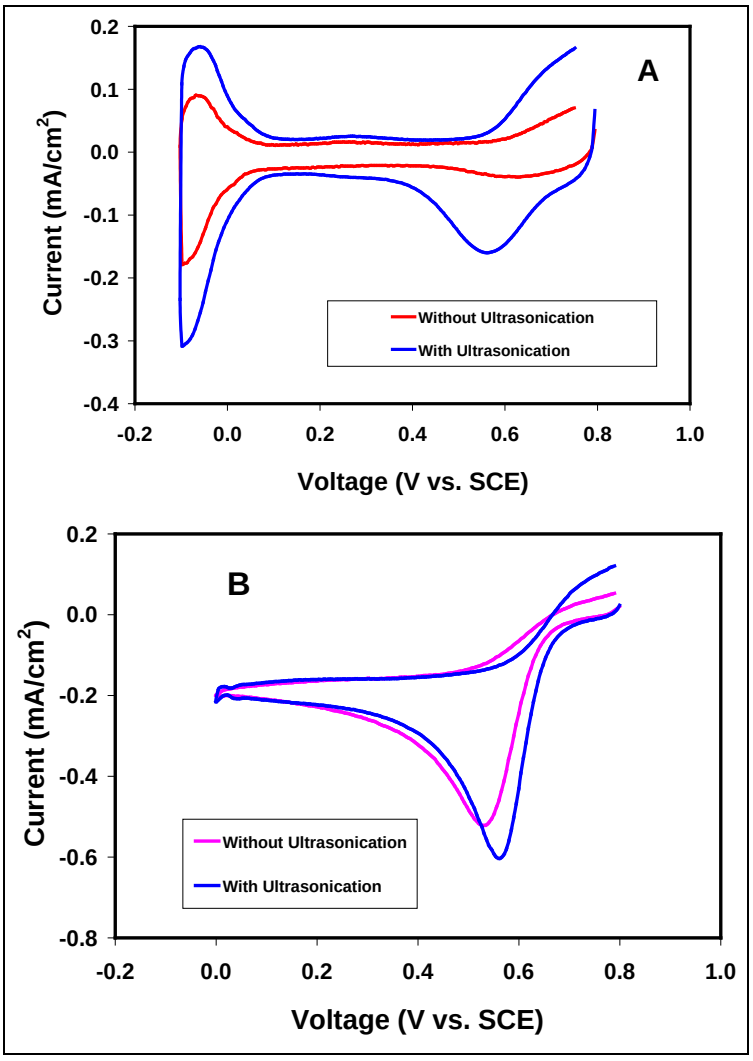

Figure 8. CVs of PtCo/GC electrodes in (a) N_2 and (b) O_2 saturated a 0.5 M H_2SO_4 solution. The scan rate was 10 mV/s. The catalysts were synthesized using U-ME-H1 and ME-H, respectively, with Pt:Co = 7:3.

3.3.2 Comparison Between Micro-emulsion and Normal Chemical Synthesis

The differences between catalytic activity for the catalysts synthesized with and without micro-emulsion are shown in figure 9. The peak current has a 110-μA/cm^2 increase for the catalyst synthesized with micro-emulsion in comparison to those synthesized using the normal method, which is relevant to decreasing particle size and increasing the active surface area. There is a 30-mV peak potential shift to positive for the catalyst synthesized with micro-emulsion, which is probably due to decreased particle size in the catalyst, and results in the increased catalytic activity.

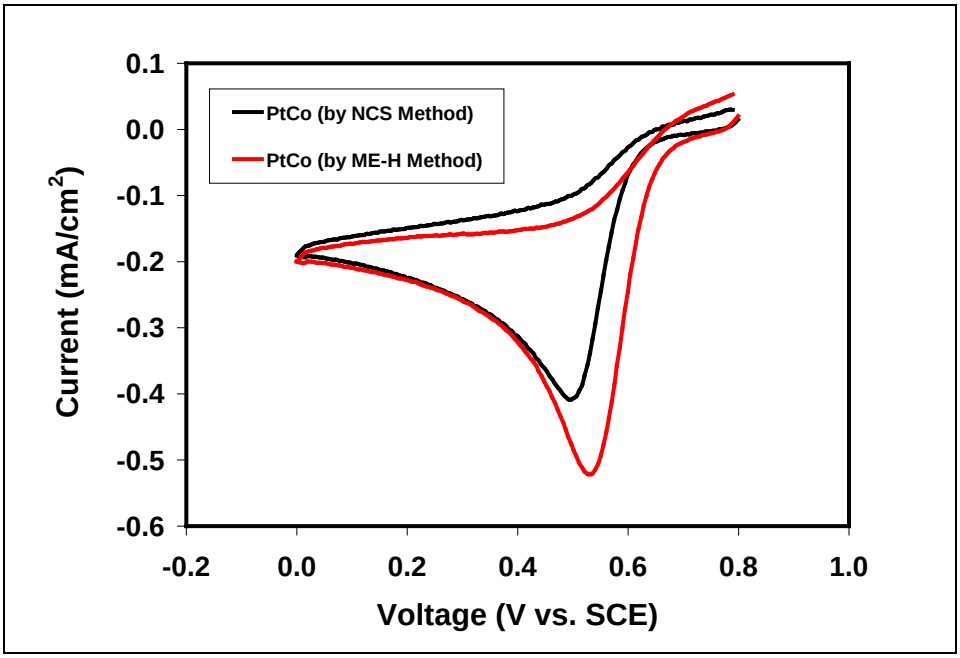

Figure 9. CVs of PtCo/GC electrodes in a O_2 saturated 0.5 M H_2SO_4 solution. The scan rate is 10 mV/s. The catalysts were synthesized by ME-H and NCS, respectively, with Pt:Co = 7:3.

3.3.3 Effect of Pt/Co ratio on Catalytic Activity

We examined the Co content in the Pt-Co catalyst on catalytic activity for oxygen reduction from zero to 40%. Figure 10 shows CVs of the PtCo/GC electrode with different Pt/Co ratios. When the ratio of Pt/Co is 7:3, the best catalytic activity was obtained. Increasing the Pt/Co ratio from 7:3 to 8:2, 9:1, and 10:0 caused the catalytic activity to decrease gradually. Likewise, decreasing the Pt/Co ratio to 6:4 also decreased the catalytic activity. This phenomenon occurs, because Pt contributes the main active sites for oxygen reduction, but Co is only an additive to enhance of the Pt's catalytic function. Co does not have catalytic activity for oxygen reduction by itself. Therefore, we focused on Pt-Co study with the 7:3 ratio in more detail.

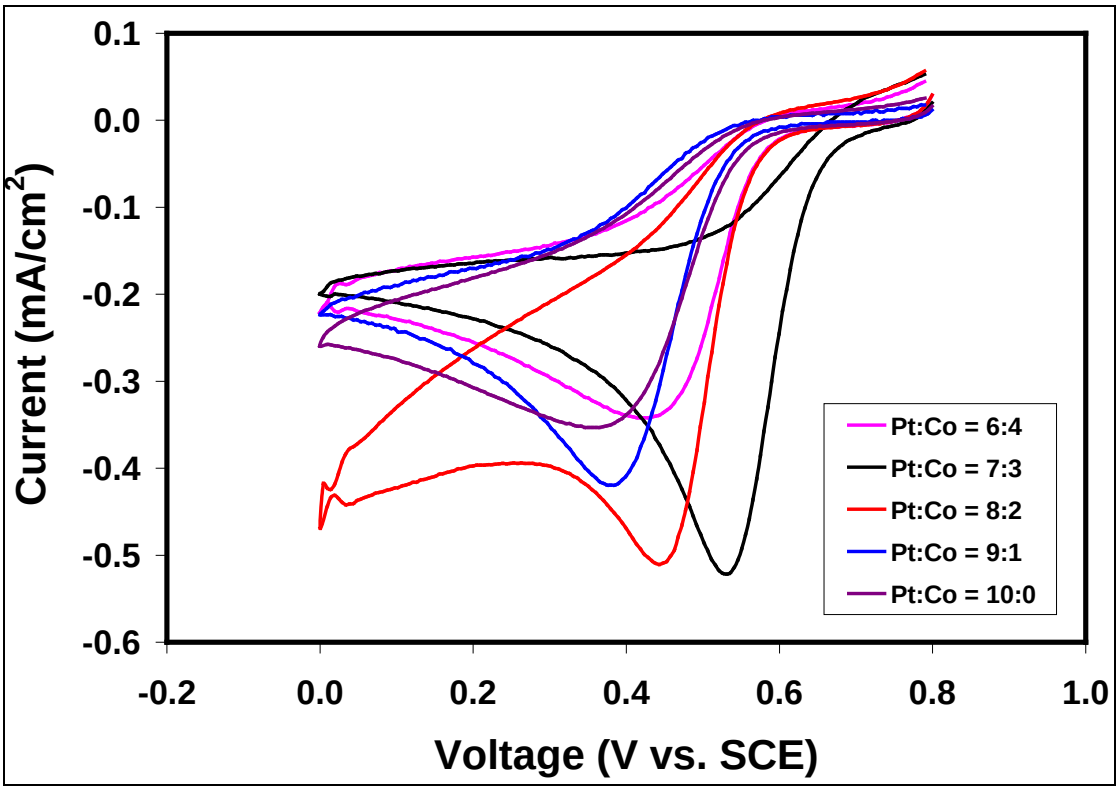

Figure 10. CVs of the PtCo/GC electrode in an O_2 saturated 0.5 M H_2SO_4 with different Pt/Co ratios. The scan rate is 10 mV/s. The PtCo was synthesized using ME-H.

3.3.4 Effect of Heat-treatment (HT) on Catalytic Activity

After micro-emulsion synthesis, HT was suggested for the catalyst, according to the literature (*30*), to remove any residual surfactant in the catalyst. However, based on our experiment, after HT, the catalyst-coated electrode showed poorer activity for catalytic oxygen reduction. Figure 11 shows CVs of the PtCo/GC electrode in an O_2 saturated 0.5 M H_2SO_4 solution that had catalysts that were either heat-treated at 200 °C or not, respectively. For the catalyst after HT, the peak potential shifted 70 mV to negative, and the peak current decreased by 180 $\mu A/cm^2$ as compared to the catalysts that were not heat-treated. This phenomenon is due to the catalyst particle size increasing after HT, especially with high temperature HT.

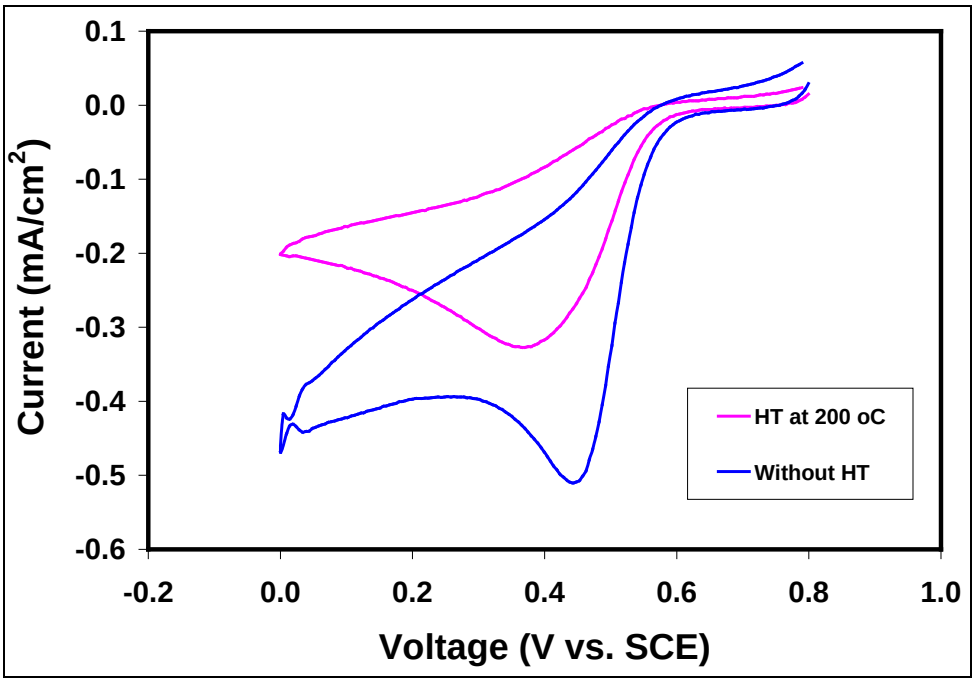

Figure 11. CVs of the PtCo/GC electrodes in an O_2 saturated 0.5 M H_2SO_4 solution. The scan rate is 10 mV/s. The catalysts were synthesized by micro-emulsion with HT at 200 °C and not heat-treated, respectively. The Pt:Co ratio was 8:2 and the synthetic method was ME-H1.

3.3.5 Compare Carbon Supported and Unsupported Catalysts

In order to save expensive noble metals, high surface area carbon was suggested as a support. Carbon supporter is useful to promote more uniform catalyst distribution. However, too much supporter will significantly dilute the active catalytic sites, resulting in lower cell performance. We needed to achieve a balance between cell performance and catalyst loading amount. Figure 12 shows CVs of the PtCo/GC and 30% carbon supported Pt/GC electrodes in an O_2 saturated 0.5 M H_2SO_4 solution. In the presence of carbon, the peak potential of the CV shifted 110 mV to negative, and the peak current increased by 90 $\mu A/cm^2$.

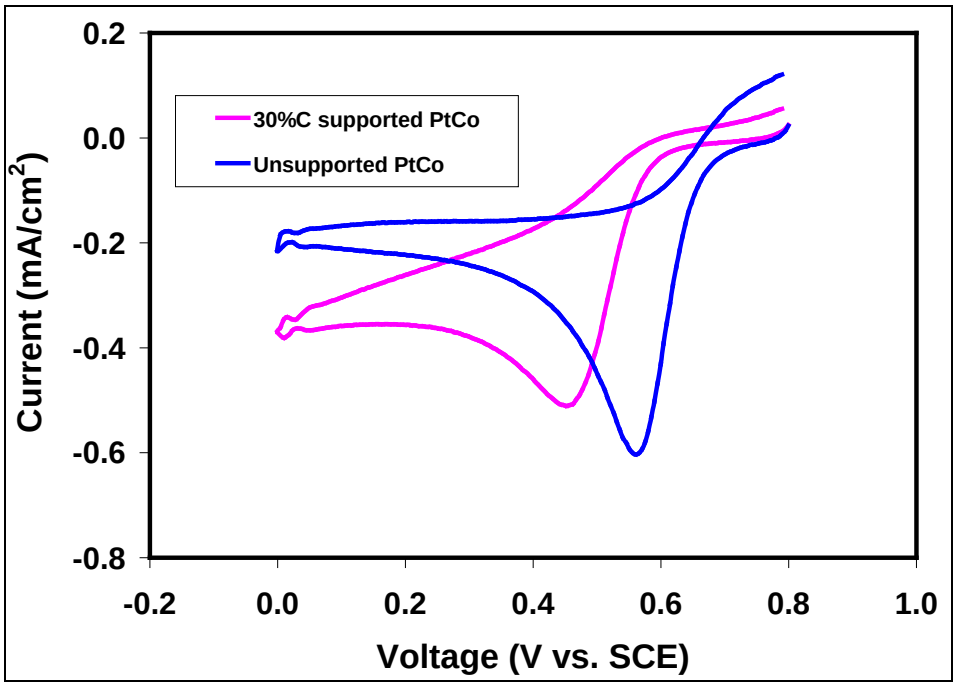

Figure 12. CVs of unsupported PtCo/GC and 30% carbon supported Pt/GC electrodes in an O_2 saturated 0.5 M H_2SO_4 solution. The scan rate was 10 mV/s and the Pt/Co ratio was 7:3. The catalysts were synthesized using U-ME-H1.

3.3.6 Effect of Sub-synthetic Methods on Catalytic Activity of Carbon Supported Catalysts

While these main synthetic methods affect the catalyst's performance, there are several other factors, or sub-synthetic methods, such as water/oil ratio, solution pH, and reactant concentration, which affect the catalytic activity appreciably. Figure 13 shows CVs of 30% carbon supported PtCo/GC in an O_2 saturated 0.5 M H_2SO_4 solution, where the catalysts were synthesized with ultrasound-assisted micro-emulsion but using different sub-methods. The catalyst synthesized with U-ME-L1 method exhibited the best catalytic activity. As shown in table 1, the U-ME-L1 method had a higher water/oil ratio, higher water/Brij ratio, and higher H_2PtCl_6 concentration than that of the U-ME-L2 method. In an attempt to decrease the size of the water droplets in the micro-emulsion, we tried to decrease the water/oil ratio. We expected that decreasing the water/oil ratio would obtain a better catalyst than it did, which implies that there may be a limit to the size of the water droplets in the micro-emulsion as one increases the oil amount. It follows that the water/Brij ratio may also determine the size of the water droplets, and in turn, determine the particles of the catalyst. Too much surfactant may increase the size of water droplets, and in turn, increase the size of catalyst particles. Comparing the U-ME-L1 and U-ME-H1 methods, the U-ME-L1 method had a lower pH in the water phase than the U-ME-H1 method due to the lack of ammonia buffer in the U-ME-L1. It seems that a lower pH in the water phase results in a smaller catalyst particle size and better catalytic performance.

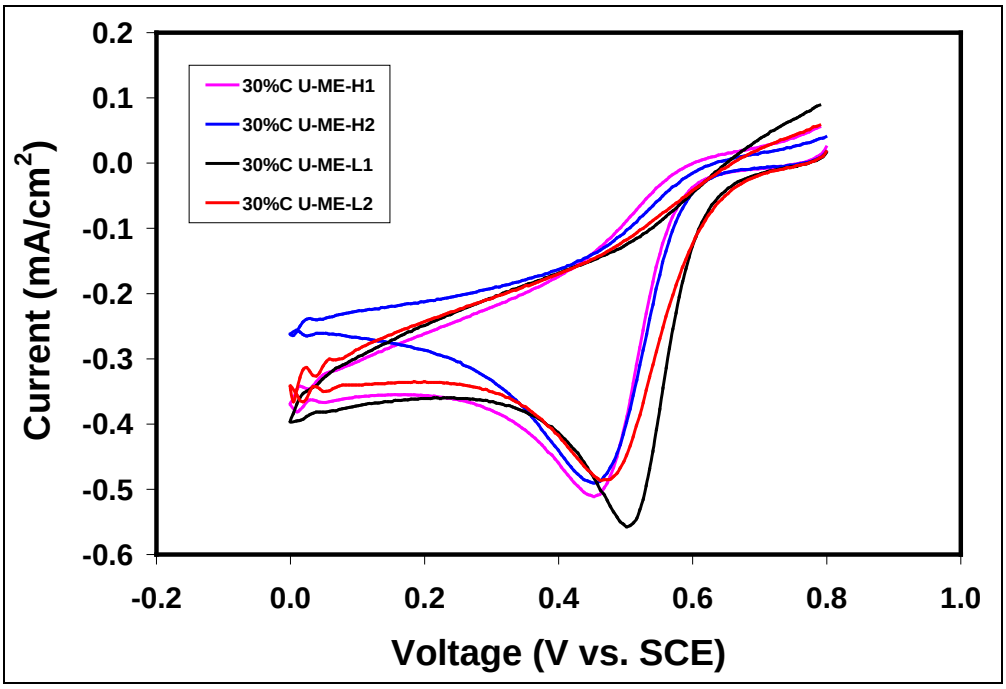

Figure 13. CVs of 30% carbon supported PtCo/GC in an O_2 saturated 0.5 M H_2SO_4 solution, where the catalysts were synthesized with ultrasound-assisted micro-emulsion but using different sub-methods. The PtCo ratio was 7:3.

3.4 Rotating Disk Electrode (RDE)

The RDE method is convenient way to measure the catalytic kinetics of an electrochemical reaction based on hydrodynamic theory. In this method, the catalyst-coated disk electrode is rotated in the electrolyte solution and the kinetic rate of the catalytic reaction is measured by varying the rotation rate. The electrode current *i* (A) on the rotating disk at a stationary state can be described using the Levich equation (equation 5) and the Koutecky-Levich equation (equation 7) (*31*),

$$i_L = 0.620nFAD_0^{2/3}\omega^{1/2}\nu^{-1/6}C_0^* \quad (5)$$

$$i_k = nFAK_f(E)Co^* \quad (6)$$

$$i^{-1} = i_k^{-1} + i_L^{-1} \quad (7)$$

$$i^{-1} = \frac{1}{nFAK_f(E)C_o^*} + \frac{1}{0.620nFAD_o^{2/3}\nu^{-1/6}C_o^*\omega^{1/2}} \quad (8)$$

Here, i_L is the Levich current for a species O's electrode reaction by a diffusion-controlled process, F (A·s) is a Faradic constant, ω (s^{-1}) is the rotation rate ($2\pi f = 2\pi \times rpm/60$), ν ($cm^2 \cdot s^{-1}$) is the viscosity of the electrolyte solution, i_k is the kinetic current of a O species at the electrode surface, and $K_f(E)$ ($cm \cdot s^{-1}$) is the rate constant at potential E. The other factors have the same meaning as described previously. The Koutecky-Levich plot, or i^{-1} versus $\omega^{-1/2}$ plot, with

equation 8, is a straight line. We can obtain a rate constant from the intercept, and a number of electron transfer in the electrode reaction from the slope with the Koutecky-Levich plot. For calculating the rate constants of a catalytic oxygen reduction, the diffusion coefficient and the concentration of oxygen in bulk solution are required. Different O_2 concentrations and diffusion coefficients were reported in the literature (*32*). In our research, we used an O_2 concentration of 1.3×10^{-6} mol/cm^3 for all calculations (*33*). A diffusion coefficient of O_2 (1.7×10^{-5} cm^2 s^{-1}) was used based on the literature (*32, 33*) for the experimental condition of a 0.5 M H_2SO_4 solution.

3.4.1 Kinetic Analysis of O_2 Reduction at PtCo/GC Electrode

Figure 14 shows polarization curves of oxygen reduction at a PtCo/GC rotating disk electrode, for which the catalyst was synthesized using ultrasound-assisted micro-emulsion. Increasing rotation rate increased the limiting current. The kinetic analysis can be analyzed using Levich and Koutecky-Levich plots. Figure 15 shows the Levich plots obtained from the data in figure 14. These plots are bent down and deviated from the straight line for an O_2 four-electron reduction by a diffusion controlled process, which indicates a kinetic controlled process. At 0.5 V, the lowest kinetic process in comparison of other electrode potentials was demonstrated.

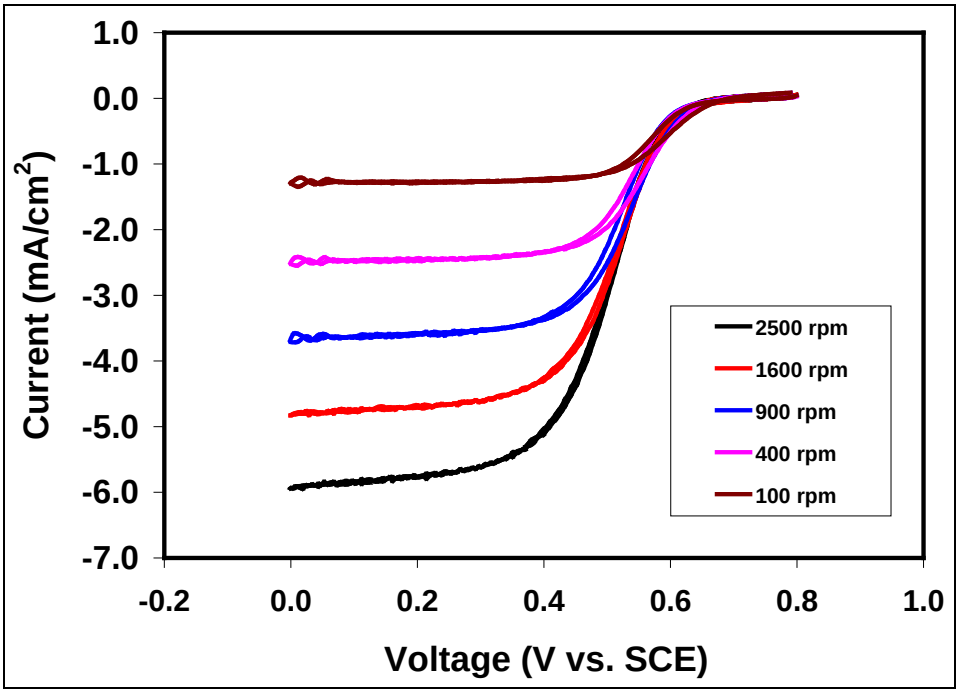

Figure 14. Polarization curves of PtCo/GC rotating disk electrode in an O_2 saturated 0.5 M H_2SO_4 solution, for which the catalyst was synthesized using ultrasound-assisted micro-emulsion at 10 mV/s with Pt:Co = 7:3.

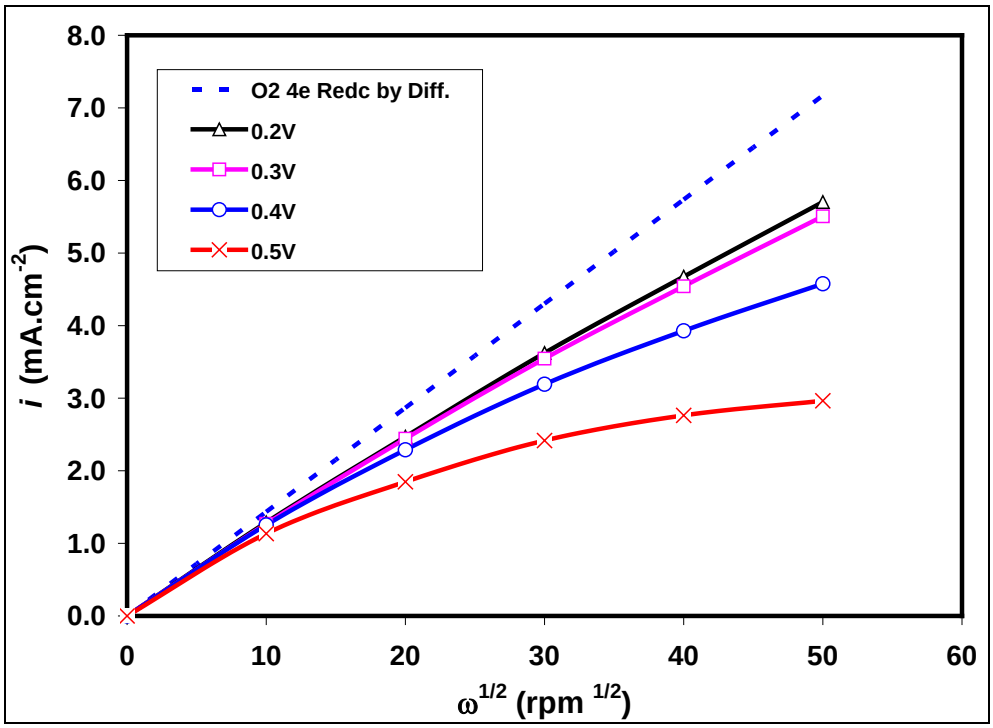

Figure 15. Levich plots obtained from the data in figure 14. The dashed line is the calculated data for an O_2 four-electron reduction by a diffusion controlled process.

Figure 16 shows Koutecky-Levich plot obtained from the data in figure 15. As expected for equation 8, all these plots are straight lines. The rate constants at different potentials are obtained and summarized in table 6. Apparently, the kinetic rate is dependent on the electrode potential. For fuel cell application, we are more interested in the kinetic rate at a high potential, such as 0.5 V (vs. saturated calomel electrode [SCE]) or 0.74 V (vs. normal hydrogen electrode [NHE]).

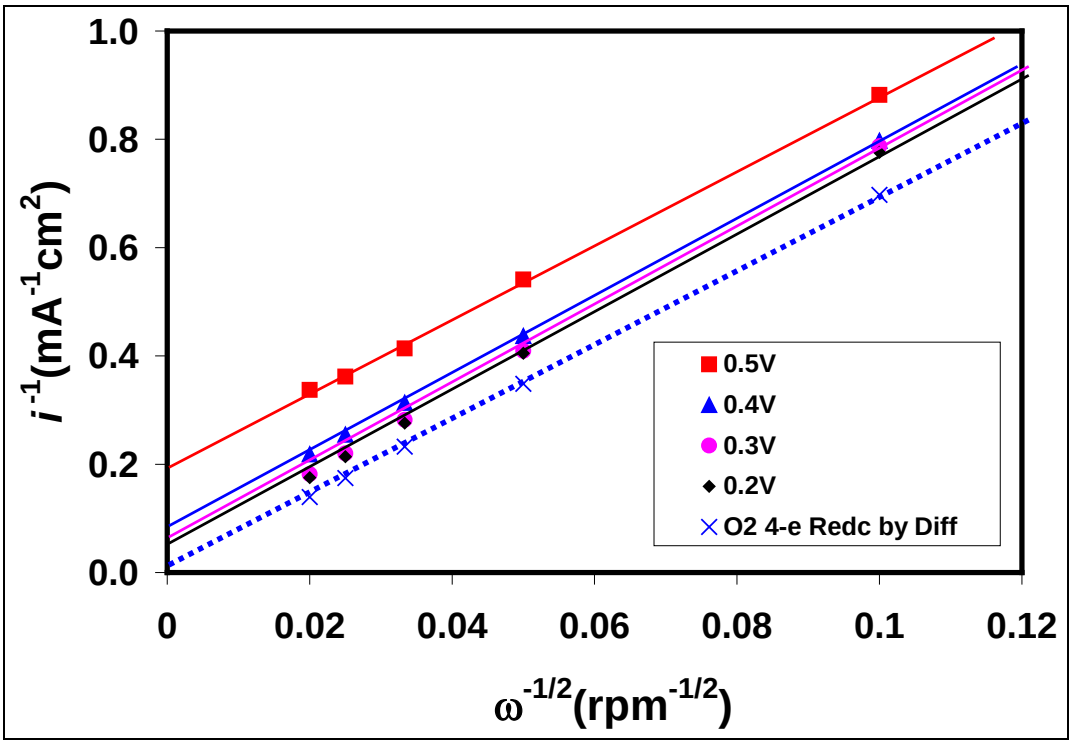

Figure 16. Koutecky-Levich plots obtained from the data in figure 15. The dashed line is the calculated data for O_2 four-electron reduction by diffusion controlled process.

Table 6. Kinetic rate constant for O_2 reduction at PtCo/GC electrode in an O_2 saturated 0.5 M H_2SO_4 solution. The catalyst was synthesized with ultrasound-assisted micro-emulsion with a PtCo ratio of 7:3.

Potential (V vs. SCE)	**Kinetic Rate Constant ($cm \cdot s^{-1}$)**
0.2	8.98×10^{-2}
0.3	6.90×10^{-2}
0.4	2.76×10^{-2}
0.5	1.09×10^{-2}

3.4.2 Effect of Synthetic Method of Catalyst on the Kinetics for O_2 Reduction

The catalysts synthesized from different methods were analyzed using the RDE method. Figure 17 shows Levich plots from the data obtained from PtCo/GC rotating disk electrodes, for which the catalysts were synthesized using different methods. The Pt-Co catalyst synthesized using ultrasound-assisted micro-emulsion showed the highest disk current at 0.5 V; its Levich plot is the top line (black).

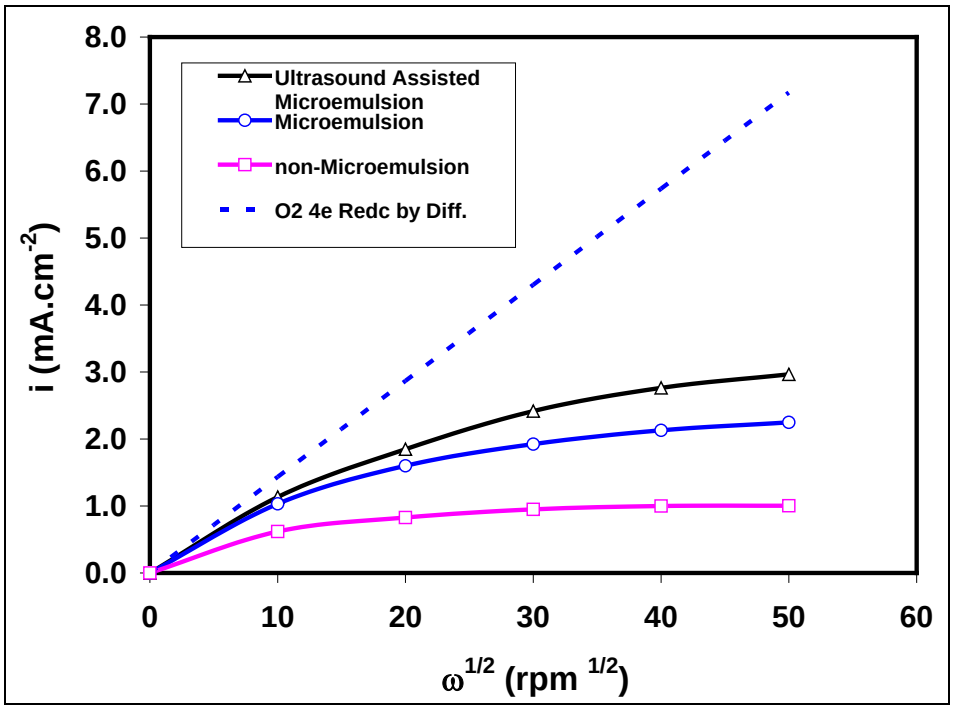

Figure 17. Levich plots obtained from PtCo/GC rotating disk electrode at 0.5 V in an O_2 saturated 0.5 M H_2SO_4 solution, for which the catalysts were synthesized using non-micro-emulsion, micro-emulsion, and ultrasound-assisted micro emulsion methods, respectively. The dashed line is the calculated data for the O_2 four-electron reduction by the diffusion controlled process.

Figure 18 shows Koutecky-Levich plots obtained from the data in figure 17. The non-micro-emulsion synthesized Pt-Co gave the highest intercept, or the slowest kinetic rate for catalytic oxygen reduction. The rate constants obtained from Koutecky-Levich plot are summarized in table 7. The kinetic rate constant of catalytic oxygen reduction for the Pt-Co catalyst synthesized using ultrasound-assisted micro-emulsion was four times higher than that of the catalyst synthesized using non-micro-emulsion.

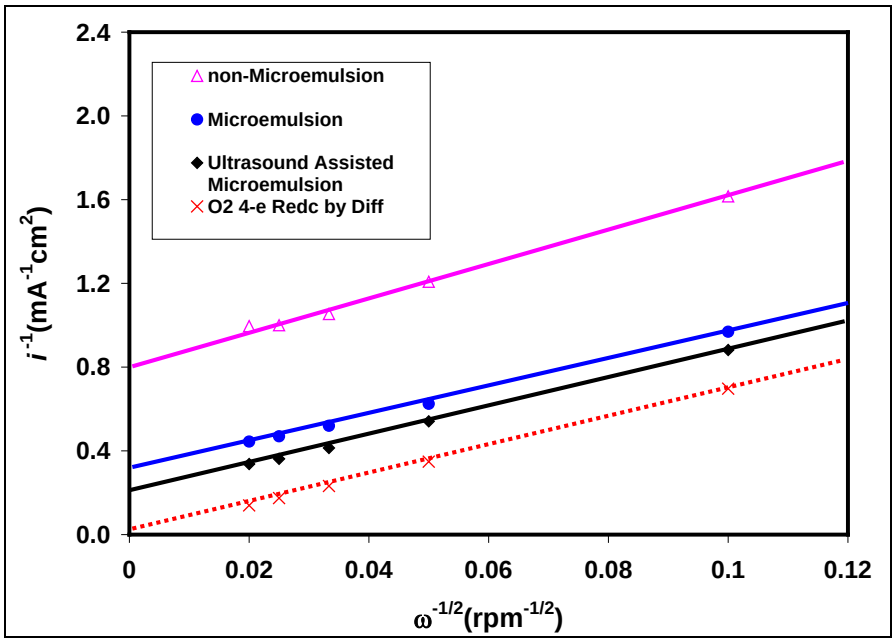

Figure 18. Koutecky-Levich plots obtained from the data in figure 17.

Table 7. Kinetic rate constant for O_2 reduction at the PtCo/GC electrode in an O_2 saturated 0.5 M H_2SO_4 solution. The catalyst was synthesized using different methods with a PtCo ratio of 7:3.

Synthetic Method	Kinetic Rate Constant ($cm \cdot s^{-1}$)
Ultrasound-assisted micro-emulsion	1.09×10^{-2}
Micro-emulsion	0.662×10^{-2}
Non-micro-emulsion	0.252×10^{-2}

3.5 Rotating Ring Disk Electrode (RRDE)

RRDE is a hydrodynamic electrochemical method for determining an intermediate product in an electrochemical reaction. In this method, the disk electrode is surrounded by a ring electrode. The intermediate product from the disk electrode can be received and determined by the ring electrode as long as an appropriate potential is applied to the ring electrode. In our research, we used the RRDE method to determine if any H_2O_2 was produced. The schemes of oxygen reduction are very complex: they can be two-electron reduced to H_2O_2, four-electron reduced to water, directly four-electron reduced to water, or two-electron reduced to H_2O_2 and then further reduced to water. Figure 19 shows the polarization curves of the PtCo/GC disk and Pt-ring electrode in an O_2 saturated 0.5 M H_2SO_4 solution, for which the catalysts was synthesized using ultrasound-assisted micro-emulsion. As expected, there was no appreciable ring current determined. We also examined the Pt-Co catalysts synthesized with other methods. There were no ring currents determined for any of the catalysts synthesized using different methods. The RRDE result demonstrated that the PtCo/GC electrode directly catalyzes an O_2 four-electron reduction to water instead of going through a H_2O_2 process.

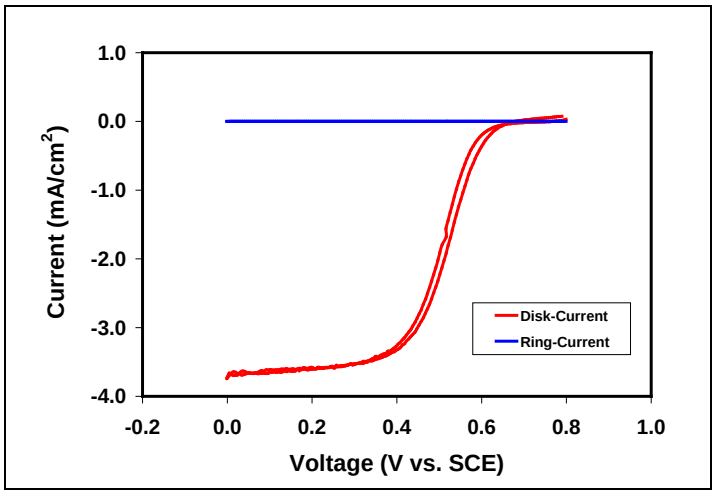

Figure 19. Polarization curves at the PtCo/GC disk and Pt-ring electrode in an O_2 saturated 0.5 M H_2SO_4 solution, for which the catalysts was synthesized using ultrasound-assisted micro-emulsion with a PtCo ratio of 7:3.

4. Conclusions

Micro-emulsion is a widely accepted method for synthesizing nano-sized catalyst particles. Our new contribution was to introduce ultrasound to the synthetic environment of the micro-emulsion synthesis. As demonstrated by TEM analysis, more uniformly distributed nano-particles of Pt-Co catalyst were obtained using ultrasound-assisted micro-emulsion synthesis. The CV results showed that by applying ultrasound-assisted micro-emulsion, the synthesized Pt catalyst experienced a 17% catalytic peak current increase for O_2 reduction over the state-of-the-art (SOA) Johnson Matthey (JM) Pt catalyst, and the synthesized Pt-Co catalyst experienced a 26% catalytic peak current increase for O_2 reduction over the SOA JM Pt catalyst. As demonstrated by the RDE method, the kinetic rate constant obtained from the Pt-Co catalyst synthesized using ultrasound-assisted micro-emulsion was four times higher than that of the same catalyst synthesized using the normal chemical method, for a catalytic oxygen reduction at 0.5 V (vs. SCE) in a 0.5 M H_2SO_4 solution. As demonstrated by the RRDE experiment, the Pt-Co catalyst coated GC electrode catalyzed an O_2 four-electron reduction to water without the intermediate product H_2O_2.

The proposed ultrasound-assisted micro-emulsion is not only applicable to Pt-Co catalyst synthesis, but could also be used to synthesize non-noble metal catalysts for fuel cell applications. Stable non-noble metal alloys could be obtained through ultrasound-assisted micro-emulsion as long as the water droplet phase that contains transition metals is buffered with ammonia to form ammonia metal complexes.

5. References

1. Steele, B.C.H.; Heinzei, A. *Nature* **2001**, *441* (6861), 345–352.
2. Appleby, A. J. *Energy* **1996**, *21* (7−8), 521–653.
3. Ren, X. M.; Zelenay, P.; Thomas, S.; Davey, J.; Gottesfeld, S. *J. Power Sources* **2000**, *86* (1–2), 111–116.
4. Conte, M.; Iacobazzi, A.; Ronchetti, M.; Vellone, R. *J. Power Sources* **2001**, *100* (1−2), 171–187.
5. Dyer, C.K.J. *Power Sources* **2002**, *106* (1−2), 31–34.
6. Rikukawa, M.; Sanui, K. *Progress in Polymer Science* **2000**, *25* (10), 1463–1502.
7. Jiang, R. Z.; Rong, C.; Chu, D. R. *J. Power Sources* **2004**, *126* (1−2), 119–124.
8. Chalk, S. G.; Miller, J. E. *J. Power Sources* **2006**, *159* (1), 73–80.
9. Kamavaram, V.; Veedu, V.; Kannan, A. M. *J. Power Sources* **2009**, *188* (1), 51–56.
10. Trogadas, P.; Ramani, V. *J. Power Sources* **2007**, *174* (1), 159–163.
11. Bonnemann, H.; Nagabhushana, K. S. *J. New Materials for Electrochemical Systems* **2004**, *7* (2), 93–108.
12. Vengatesan, S.; Kim, H. J.; Kim, S. K.; et al. *Electrochimica Acta* **2008**, *54* (2), 856–961.
13. Zhang, L.; Lee, K. C.; Zhang, J. J. *Electrochimica Acta* **2007**, *52*, 7964–7971.
14. Min, M.; Park, C.; Kim, H.; et al. *Electrochimica Acta* **2006**, *52*, 1670–1675.
15. Li, G. H.; Hu, L. J.; Hill, J. M. *Applied Catalysis A-General* **2006**, *301* (1), 16–24.
16. Lebedeva, N. P.; Janssen, G.J.M. *Electrochimica Acta* **2005**, *51* (1), 29–40.
17. Siracusano, S.; Stassi, A.; Baglio, V.; et al. *Electrochimica Acta* **2009**, *54* (21), 4844–4850.
18. Malheiro, A. R.; Perez, J.; Villullas, H. M. *J. Electrochem. Soc.* **2009**, *156* (1), B51–B58.
19. Luna, A.M.C.; Bonesi, A.; Triaca, W. E.; et al. *J. Solid Satate Electrochem.* **2008**, *12* (5), 643–649.
20. Wang, X.; Hsing, I. M. *Electrochimica Acta* **2002**, *47* (18), 2981–2987.
21. Raghuveer, V.; Ferreira, P. J.; Manthiram, A. *Electrochemistry Communications* **2006**, *8* (5), 807–804.

22. Hayashi, M.; Uemura, H.; Shimanoe, K.; et al. *J. Electrochem. Soc.* **2004**, *151* (1), A158–A163.

23. Liu, Z.; Yu, C.; Rusakova, I. A.; Huang, D.; Strasser, P. *Top Catal* **2008**, *49*, 241–250.

24. Coutanceau, C.; Brimaud, S.; Lamy, C.; Leger, J. M.; Dubau L.; Rousseau, S.; Vigier, F. *Electrochimica Acta* **2008**, *53*, 6865–6880.

25. Zeng, J.; Lee, J.Y.J. *Power Sources* **2005**, *140*, 268–273.

26. Uchida, H.; Izumi, K.; Watanabe, M. *J. Phys. Chem. B* **2006**, *110*, 21924–21930.

27. Yano, H.; Song, J. M.; Uchida, H.; Watanabe, M. *J. Phys. Chem. C* **2008**, *112*, 8372–8380.

28. Bard, A. J.; Faulkner, L. *Electrochemical Methods, Fundamentals and Applications*; John Wiley & Sons, New York, 1980, pp 218–222.

29. Schulenburg, H.; Muller, E.; Khelashvili, G.; Roser, T. H.; Bonnemann, H.; Wokaun, A.; Scherer, G. G. *J. Phys. Chem. C* **2009**, *113*, 4069–4077.

30. Bard, A. J.; Faulkner, L. *Electrochemical Methods, Fundamentals and Applications*; John Wiley & Sons, New York, 1980, pp 288–291.

31. Itoe, R. N.; Wesson, G. D.; Kalu, E. *J. Electrochem. Soc.* **2000**, *147*, 2445.

32. Jiang R. Z.; Anson, F. C. *J. Electroanal. Chem.* **1991**, *305*, 171.

6. Transitions

We plan to transition the proposed method of using ultrasound-assisted micro-emulsion for synthesizing nano catalysts to our mission work in synthesizing stable non-noble metal alloys for alkaline fuel cells. The results obtained in the FY09 DRI research are also planned for publication in peer-reviewed journals.

List of Symbols, Abbreviations, and Acronyms

ARL	U.S. Army Research Laboratory
ASR	Adjustable Speed Rotator
Co	cobalt
$CoCl_2 \cdot 6H_2O$	cobalt (II) chloride hexahydrate
CV	cyclic voltammetry
DRI	Director's Research Initiative
EDS	energy dispersive x-ray spectroscopy
GC	glassy carbon
$H_2PtCl_6\ 5H_2O$	hydrogen hexachloro-platinum pentahydrate
H_2SO_4	sulfuric acid
HT	heat-treatment
JM	Johnson Matthey
ME-H	micro-emulsion in high pH environment
ME-L	micro-emulsion in low pH environment
N_2	nitrogen
$NaBH_4$	sodium borohydride
NCS	Normal Chemical Synthesis
NH_4OH	ammonium hydroxide
O_2	oxygen
Pt	platinum
PtCo/GC	Pt-Co coated GC electrode
RDE	rotating disk electrode
RRDE	rotating ring disk electrode
SCE	saturated calomel electrode

SOA	state-of-the-art
TEM	transmission electron microscope
U-ME-H	ultrasound-assisted micro-emulsion in high pH environment
U-ME-L	ultrasound-assisted micro-emulsion in low pH environment
XRD	x-ray diffraction analysis

No. of Copies	Organization
1 ELEC	ADMNSTR DEFNS TECHL INFO CTR ATTN DTIC OCP 8725 JOHN J KINGMAN RD STE 0944 FT BELVOIR VA 22060-6218
1 CD	US ARMY RSRCH LAB ATTN RDRL CIM G T LANDFRIED BLDG 4600 ABERDEEN PROVING GROUND MD 21005-5066
3 CDS 6 HCS	US ARMY RSRCH LAB ATTN IMNE ALC HRR MAIL & RECORDS MGMT ATTN RDRL CIM L TECHL LIB ATTN RDRL CIM P TECHL PUB ATTN RDRL SED C DR. CHARLES RONG (3 HCS) ATTN RDRL SED C DR. RONGZHONG JIANG (3 HCS) ADELPHI MD 20783-1197

TOTAL: 11 (1 ELEC, 4 CDS, 6 HCS)